IAC–18–C1.8.7

OPTIMAL ESCAPE MANIFOLDS FOR CIS-LUNAR HALO ORBITS

Lorenzo Bucci
Politecnico di Milano, Italy
lorenzo.bucci@polimi.it

Andreas Kleinschneider
ESA-ESOC, Germany
andreas.kleinschneider@esa.int

Michèle Lavagna
Politecnico di Milano, Italy
michelle.lavagna@polimi.it

Florian Renk
ESA-ESOC, Germany
florian.renk@esa.int

Different families of three-body orbits are being proposed as location for a human-tended lunar orbiting station, and as operational orbit for communication relay and navigation satellites. In particular, Space Agencies are currently considering the Near Rectilinear Halo Orbits (NRHO) family as a staging location for a lunar exploration infrastructure. Due to the increased interest, a close investigation of the NRHO dynamics, at insertion and departure respectively, is worth to consolidate transfer capabilities, back and forth the Earth and other destinations. The paper investigates the trajectory sensitivity to the incoming and outgoing manoeuvres direction; different models (Circular Restricted Three-Body Problem, Bi-Circular Restricted Four-Body Problem, full ephemeris model) are exploited, to gradually increase fidelity of the dynamical model and to classify the transfer shape. For any manoeuvre direction, several manifolds for NRHO departure/arrival exist, differing in manoeuvre magnitude and time of flight.
The initial aim of the investigation was to search for escape trajectories that exploit Weak Stability Boundary (WSB) dynamics, to obtain a low energy ballistic capture. Generally, a single family of trajectories directly leaves the NRHO towards the WSB. The other manifolds describe additional orbits around the Moon before connecting to the WSB, either going towards heliocentric escape, or colliding with the Moon or the Earth. Notably, the correlation between time of flight and manoeuvre magnitude is highly irregular; Finite Time Lyapunov Exponents (FTLE) are here used to correlate the two quantities to identify transitions between dynamical regimes, in order to derive the manoeuvres bounds that describe similar dynamical behaviours. To deepen the knowledge of the dynamical regime, the paper analyses the manoeuvre direction effect, mapping the results in Azimuth-Elevation plane with respect to the Earth-Moon rotating frame. Optimal Δv directions are identified, as circular structures in such phase space, whose bounds are defined through a local FTLE analysis; this offers the analyst a further degree of freedom in manoeuvre planning, e.g. to satisfy pointing constraints.
As operational example, WSB transfers from/to Earth are identified, showing how a proper exploitation of the manifold structures and geometry can reduce the magnitude of said manoeuvres. Theperformed analyses give rise to general guidelines for manoeuvres design; indeed, transfers to and from any Halo orbit - optimal in terms of manoeuvre magnitude and time of flight - can be easily assessed.

1. Introduction

The investigation of the dynamical space, in the neighbourhood of libration point orbits, is a topic of growing interest in astrodynamics and trajectory design domains [1, 2].

The knowledge of the dynamical flow in proximity of the cis-lunar space enables advanced techniques for orbits design, station-keeping, transfer strategy definition, improving the comprehension of the complex and chaotic nature of the Earth-Moon system.

Recent studies introduced the use of dynamical systems theory in astrodynamics problem [3, 4, 5]. Namely, chaos and chaotic systems theory are applied to non-Keplerian regimes, to investigate the phase-space of libration point orbits and help mission design. The main aim of said studies is to deepen the knowledge of the high non-linearities of the environment, and to give novel results to the astrodynamics investigations by borrowing dynamical systems theory tools.

The paper proposes an investigation of the cis-lunar Halo orbit escape/capture dynamics; assuming to perform a manoeuvre, the effect of magnitude and direction is investigated, proposing the use of Finite Time Lyapunov Exponents to identify boundaries in the phase space, aiming at an identification of possible optimal escape manifolds. The same approach, with backwards integration in time, allows to identify capture manifolds and dynamics.

The different dynamical models and mathematical tools, employed throughout the study, are presented in Section 2; in particular, a new scalar measure is introduced, to quantify and classify the different dynamical behaviours observed. Section 3 proceeds with the core of the investigation, mapping the solution space and identifying the possible solution families. An operational example is offered in Section 4, showing a converged WSB transfer which employed the mapping techniques to generate initial guess. Section 5 concludes the paper, wrapping up the results and providing suggestions for future studies.

2. Model and assumptions

2.1 Equations of motion

The starting point for Halo orbits investigation is often the Circular Restricted Three-Body Problem (CR3BP). This model assumes a spacecraft, with negligible mass, to be moving under the gravitational pull of two massive bodies, which mutually revolve in circular orbits [6].

$$\ddot{x} - 2\dot{y} = U_x \tag{1}$$

$$\ddot{y} + 2\dot{x} = U_y \tag{2}$$

$$\ddot{z} = U_z \tag{3}$$

Equations 1-3 describe the dynamics of the spacecraft in the CR3BP framework, employing dimensionless, barycentric coordinates. The partial derivatives U_x, U_y, U_z are referred to the potential function

$$U = \frac{1}{2}(x^2 + y^2) + \frac{1-\mu}{r_1} + \frac{\mu}{r_2} \tag{4}$$

where r_1 and r_2 denote the magnitudes of $\mathbf{r}_1$ and $\mathbf{r}_2$, the distances of the spacecraft from the two primaries. As the fidelity of the model needs to be increased, the Elliptic Restricted Three-Body Problem (ER3BP) may be employed, with a similar formulation and nomenclature, but taking into account the eccentricity of the relative orbit between the two primary bodies [7].

Some of the trajectory analysed in the paper, namely, the Weak Stability Boundary transfers [8, 9], are based on the exploitation of the gravitational pull of the Sun, together with the Earth and the Moon. Thus, both three-body problem formulations are not suitable for such kind on study, and the Sun gravity shall be added to the model. The Bi-Circular Restricted Four-Body Problem (BCR4BP) is an efficient model to take into account Earth, Moon and Sun gravities [1], with a reduced increase in complexity. Within the BCR4BP, equations 1-3 are modified by adding the time-dependent gravitational pull of the Sun, assumed to move circularly in the Earth-Moon plane

$$\ddot{x} - 2\dot{y} = U_x - \frac{\mu_s}{r_s^3}(x - x_s) - \frac{\mu_s}{a_s^3}x_s \tag{5}$$

$$\ddot{y} + 2\dot{x} = U_y - \frac{\mu_s}{r_s^3}(y - y_s) - \frac{\mu_s}{a_s^3}y_s \tag{6}$$

$$\ddot{z} = U_z \tag{7}$$

Equations 5-7 describe the motion of a massless spacecraft in the BCR4BP; note that the two additional terms, in the planar components, may be seen as a perturbation of the CR3BP [10]:

- The first term indicates the direct gravitational pull of the Sun on the spacecraft;
- The second term derives from the Earth-Moon barycentre acceleration, due to the Sun gravity.

At early stage of the research, the investigation was carried out with the restricted models; the results presented in the paper are eventually obtained with a full ephemeris model, employing the real position of Sun, Earth and Moon with the JPL DE405 model.

2.2 Orbit strain index

The present investigation deals with trajectories that originate from/to non-Keplerian Halo orbits, but do not strictly belong to an orbit family. Furthermore, the distinction between given trajectories might be clear by visual shape inspection, but the numerical implementation needs a value to work with. Thus, the necessity of identifying some parameters

arises, in order to give a measure, at least qualitative, of how the orbit is modified. A parameter is here proposed, which indicates how the orbit elongates in respect to its nominal shape.

Let us consider the physical length of an orbit in space

$$L(T) = \int_0^T \mathbf{x}(t)\ ds \tag{8}$$

The nominal value, L_0, is taken as reference; the measure of expansion of the orbit ϵ, due to a perturbation, may be computed through a structural mechanics analogy, as the natural logarithm of the ratio between dilated and nominal length (i.e., the strain of the orbit), as defined in equation (9)

$$\epsilon(t) = \log \frac{L(t)}{L_0} \tag{9}$$

Previous studies [11, 12] employed a momentum integral as escape performance, with application to station-keeping and disposal trajectories. Such index, although different from the orbit strain employed in the current investigation, leads to the same conclusions about the dynamical flow in cis- and translunar non-Keplerian orbits. In general, any performance index that monitors the elongation of the state flow (i.e. integrals that involve position and/or velocity) may be employed for an escape analysis.

2.3 Finite Time Lyapunov Exponents (FTLE)

The concept of Lyapunov exponents derives from Lyapunov's stability theory. Successive early studies [13] provide a mathematical description, within the context of dynamical system theory, until recent works [3, 5] which describe their use in astrodynamics problems. Recalling the specialized literature for a detailed description, the Finite Time Lyapunov Exponents (FTLE) are here defined as

$$\Lambda(t) = \frac{1}{|t|} \log(\max(\mathrm{eig}\sqrt{J^T J})) \tag{10}$$

Equation (10) employs the following nomenclature:

- $\Lambda(t)$ is the FTLE at the time instant t.
- The matrix J is the Jacobian of the dynamical system at hand, defining the variation of a given quantity with respect to a variation in the independent variables. In general, J may not be square.

At first inspection, the FTLE does not possess a straightforward meaning, as it involves the maximum eigenvalue of a matrix which has no direct relation to the state. If the STM of the system is used [3], the FTLE will indicate the strain of the phase-space flow. In the current investigation, the concept of FTLE was extended beyond the state representation, employing a more general definition which relies on the problem Jacobian. Note that the STM may be interpreted naturally as the Jacobian of the final state with respect to the initial state, thus no generality is lost in the definition here employed.

3. Solution space investigation

In this Section, the main results of the study are presented. As working bench, the faminly of Near Rectilinear Halo Orbits (NRHO).

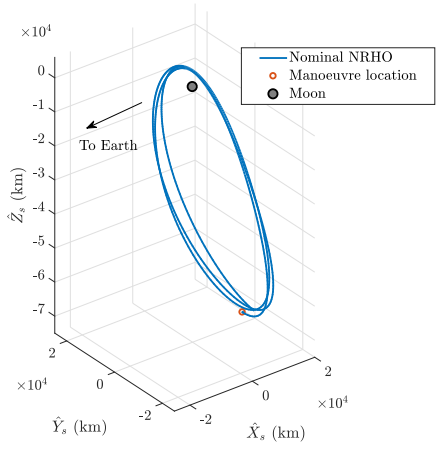

Figure 1: Sample NRHO and manoeuvre location in Earth-Moon rotating frame

The large search-space is narrowed down as follows:

- A manoeuvre is performed at the orbit aposelene. Although restricting, this assumption allows a preliminary investigation of the dynamical portraits without loss of generality.
- The epoch of the manoeuvre is fixed. Since the investigation is carried out in the Earth-Moon rotating frame, changing the epoch implies a change in the relative Earth-Moon-Sun geometry, thus modifying the acceleration field. The epoch may be considered as additional parameter, although the direction study is meaningful if performed at the same initial epoch.

- The magnitude of the manoeuvre is limited to 20 m/s. As the magnitude is increased, self-similar patterns are observed in the solution.

Figure 1 summarizes the investigation geometry; the approach may be naturally extended to any other non-Keplerian orbit in cis-lunar space.

The manoeuvre direction is parametrized in spherical coordinates, with the nomenclature of Figure 2, in the Earth-Moon rotating frame.

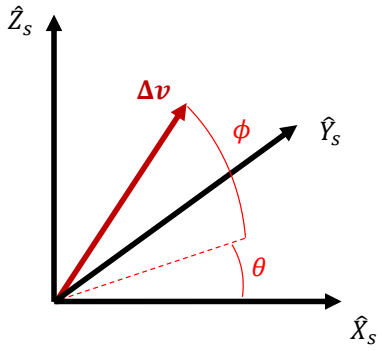

Figure 2: Spherical coordinates nomenclature

3.1 Optimal manoeuvre direction

Let us consider to apply a planar manoeuvre, in the Earth-Moon rotating frame, at the aposelene of an NRHO, and to compute the orbit strain index ϵ at the end of the integration. Running a parametric analysis, varying the manoeuvre magnitude and direction, allows to portray maps of the strain index, investigating the solution space.

Figures 3 and 4 depict the strain index, ϵ, obtained for different values of Δv and azimuth θ; the trajectory is numerically integrated for 120 days, forward and backwards in time. The resulting maps allow to understand the transitions between dynamical regimes; although the orbit strain has no direct meaning, and no information about the actual trajectory shape is retrieved, these maps are useful to identify chaotic transition regions. The contour plots are created with a bold, black line at the edges; by doing so, peaks and sudden variations in the contour surface result in black-scattered regions, whereas smooth transition are portrayed with a continuous black line.

The FTLE may be employed as a measure of sensitivity, and will be itself affected by the chaotic nature of the solution. Figure 5 depicts the FTLE related to Figure 3; note how the patterns of the two figures are

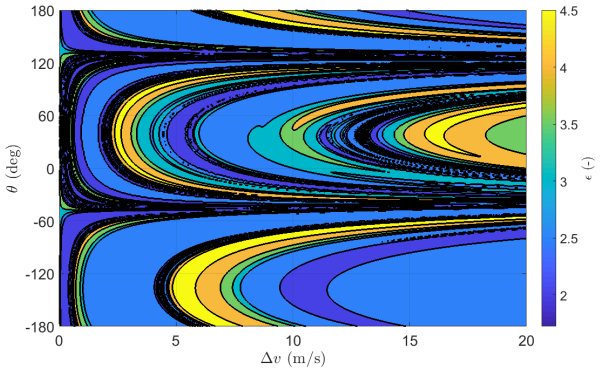

Figure 3: Azimuth-Δv map, forward integration for 120 days

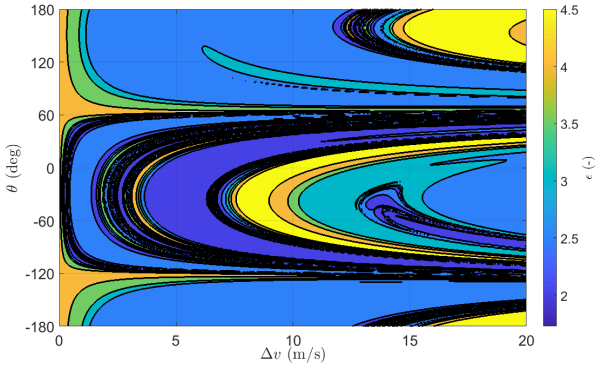

Figure 4: Azimuth-Δv map, backwards integration for 120 days

similar, although representing different behaviours. Recalling the definition of FTLE in equation 10, the Jacobian of the problem is here defined as

$$J = \frac{\partial \epsilon}{\partial \boldsymbol{\eta}} \quad \text{with} \quad \boldsymbol{\eta} = [\Delta v \ \theta]^T \tag{11}$$

In general, chaotic transitions are difficult to describe from a quantitative point of view, whereas visual aid techniques [3] may be employed. Within the current work:

- The black ridges in Figures 3 and 4 help to identify chaotic transitions between dynamical regimes;
- The FTLE gives an index of the sensitivity of the solution, and manifests as well a chaotic behaviour in transition regions.

The optimal manoeuvre direction, for a given direction, may be identified as follows:

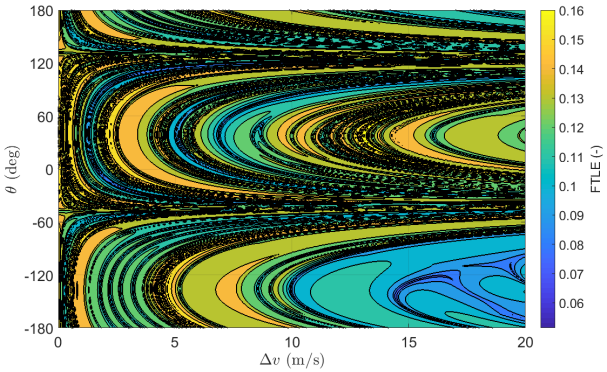

Figure 5: Azimuth-Δv Lyapunov exponent map of Figure 3

1. Start at a point with given coordinates $\Delta v, \theta$ that yields the desired dynamical behaviour; e.g., let us consider an escape trajectory with $\Delta v = 13$ m/s and $\theta = -66$ deg, in Figure 3.

2. A given orbit strain index will be associated with such behaviour, within the bound dictated by the black ridges; e.g., the yellow region in the lower right-hand side.

3. For any value of ϵ, it is possible to move leftward, following the contour colour, until a point with minimum Δv is reached, within the same region; e.g. $\Delta v = 5.5$ m/s and $\theta = -136$ deg.

Figure 6 shows the self-similar trajectories, along the yellow region employed in the description. Although different, all the trajectories show the same macroscopic dynamical behaviour, thus proving the effectiveness of the orbit strain index ϵ and the existence of optimal direction, given the desired dynamical behaviour.

Such statement is linked to the relative Earth-Moon-Sun geometry at the manoeuvre epoch: trivially, the weakly-bounded dynamics of Halo orbits is sensitive to the Sun perturbation, whose location at the initial epoch dictates the optimal direction for escape, as noted also in a contemporary study [12]. The novelty here introduced is the investigation of self-similar patterns, exploring how the optimal direction may be found by starting from non-optimal solution, mimicking the desired dynamical behaviour. As noted in the following Sections, such technique may be employed to investigate different problems, classifying the solutions into families, and generating initial guesses for local optimizers.

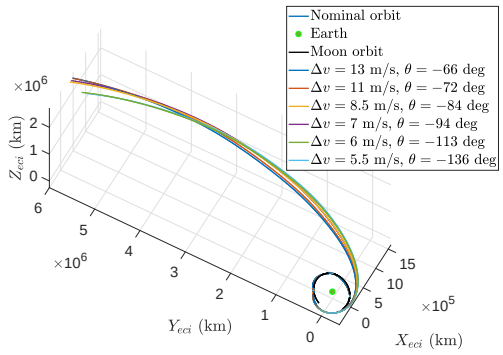

Figure 6: Self-similar escape solutions

3.2 In-plane vs. out-of-plane

The present Section investigates the possible advantages of an out-of-plane manoeuvre.

Figure 7 portrays a map, that indicates how the strain ϵ varies with the azimuth and elevation angles, for a fixed magnitude of the manoeuvre.

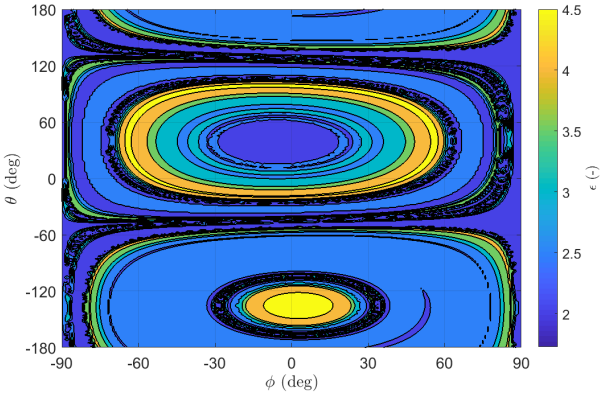

Figure 7: Azimuth-elevation map, $\Delta v = 5$ m/s

A circular, symmetric pattern may be noted in the map. Recall that the orbit strain index, ϵ, is not to be taken as a figure of merit per se, but is exclusively employed to identify self-similar patterns and behaviours in the dynamical space. The presence of circular patterns allows to conclude that, if a given dynamical behaviour is obtained with an out-of-plane manoeuvre, there will always exist an in-plane manoeuvre which will yield the same behaviour. The line crossing the null elevation angle, $\phi = 0$, includes any possible strain index of the map. Naturally, there is no a priori guarantee that the trajectories will be exactly coincident, but only conclusions regarding their self-similarity.

A preliminary hypothesis for the presence of circular patterns lies in the existence of the Coriolis apparent acceleration in the xy plane. The deviation of the trajectory from the nominal one is, mainly, due to this acceleration, and thus dominated by the in-plane behaviour.

3.3 Solution families

As noted previously, it is possible to identify self-similar trajectories, which are obtained from different combinations of Δv and θ, assuming null elevation angle. To identify solution families, a cut in the solution surface is performed, along the line corresponding to the optimal direction. As operational example, let us consider to cut Figure 3 along the $\theta = 37$ deg line. The main topic of the current investigation was the search for escape direction, targeting heliocentric orbits or Earth reentry with low-energy manoeuvres.

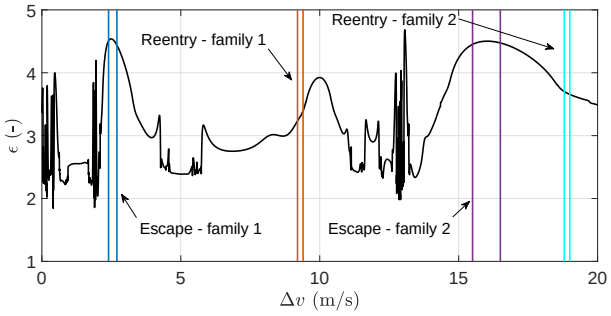

Figure 8: Cut at $\theta = 37$ deg

The orbit strain index is not able to give information about the shape of the trajectory; nevertheless, it is possible to state that, in the regions where the strain index is similar, between the boundaries dictated by the chaotic regions and FTLE peaks, all the solutions will manifest similar behaviour, and may thus classified into a family. Let us proceed by visual inspection of Figure 8, which shows the cut of Figure 3 along the $\theta = 37$ deg line.

- The first peak is associated with a solution family. Although not foreseeable a priori, computing the distance from the Earth allows us to note that this family corresponds to heliocentric escape behaviours.

- Then, we sample an orbit before the second peak, prior to a small chaotic transition. This region corresponds to Earth ballistic reentry, as noted again after computation of the Earth distance.

- Going on in the analysis of different regions, we may identify other reentry and escape families; although outside the scope of the current investigation, different dynamical patterns are present in the vast phase space.

Figure 9 depicts the distance from the Earth, for the corresponding identified families, where the ballistic reentry and escape dynamics are evident. Note that the first families (labelled with 1, associated with lower Δv) leave the NRHO regime after roughly 40 days, whereas the second families (labelled with 2, associated with higher Δv) depart after 28 days. Different, independent studies [12] observed the same pattern, classifying the trajectories according to the number of revolutions prior to departure. It is remarked that the present analysis was limited to low values (less than 20 m/s) of Δv magnitude; as such value is increased, the self-similarity of the problem will reveal more and more, enabling the identification of escape/reentry patterns after shorter amounts of time.

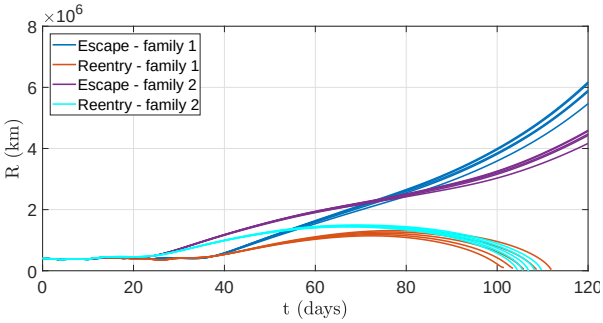

Figure 9: Distance from Earth for different families

A close-up view of the departure from NRHO is portrayed in Figure 10, where the different behaviours can be appreciated. In particular, the trajectory twirls prior to departure are notable, as they lead to similar long term trajectories after different amounts of time. Eventually, Figure 11 depicts the selected solution families in a Earth-centred inertial frame, where the reentry and escape dynamics are clear. The ballistic reentry trajectories correspond to Earth capture after I or III quadrant weak-stability boundary transfer, whereas the escape trajectories are related to prograde or retrograde heliocentric escape.

The same trajectory patterns and dynamical behaviours may be obtained by backwards integration, as the same consideration apply. By performing a cut in Figure 4, one may compute trajectories that lead,

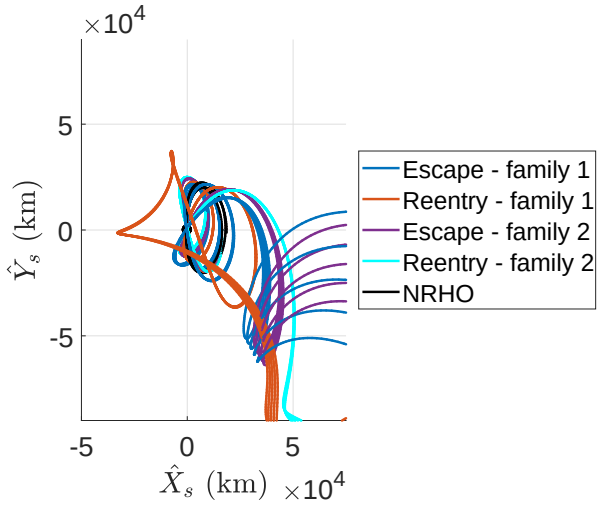

Figure 10: Sample solution families, initial segments in Earth-Moon rotating frame

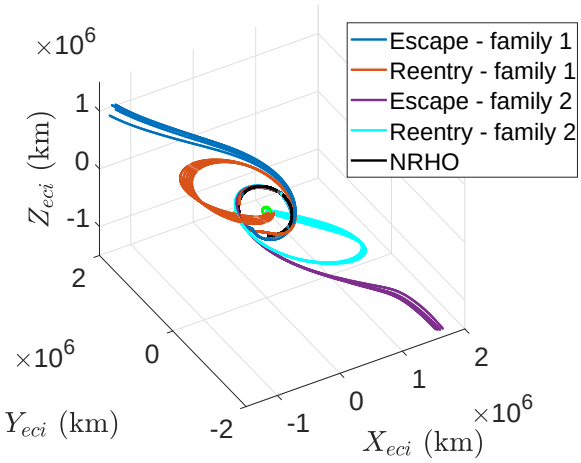

Figure 11: Sample solution families, Earth-centred inertial frame

e.g., to a quasi-ballistic NRHO capture, deriving from a lunar-bound transfer orbit or from an incoming hyperbola after an interplanetary arc.

4. Case study: WSB transfer

The existence of preferable manoeuvre directions was shown in the previous Sections. In the following, their use to efficiently generate first guess trajectories is illustrated. This section begins with a short qualitative description of WSB transfers. An example scan of manoeuvre directions is discussed to underline the applicability of above's discussion for WSB trajectory design, using transfers to an NRHO as example.

4.1 WSB transfers and generation

WSB transfers employ the Sun's gravity gradient to reduce Δv costs as compared to a direct transfer. Considering a transfer from Earth orbit to an NRHO, the typical saving is around 150 m/s, and can be even higher for other libration point orbits. However, the typical transfer time via WSB is in the order of months compared to days for direct transfer options.

To follow a WSB transfer to an NRHO the geocentric apogee has to be raised well beyond the Moon's orbit, to approximately 1.4 million kilometers. In this WSB region, the Sun's gravity gradient has a considerable effect on the orbit. If the apogee is in the second or fourth quadrant with respect to the Sun the gravity gradient accelerates the spacecraft, raising the orbit perigee.

By varying the parameters of the transfer and adding a small burn at apogee the perigee can be chosen such that the spacecraft arrives at or near the targeted lunar orbit. In principle it is possible to find a fully natural transfer, not requiring any manoeuvre at apogee. However, depending on the desired launch window, target orbit, and Earth departure orbit, a deterministic WSB manoeuvre is necessary. Typical values range in the tens of m/s, but can be in the hundreds of m/s for unfavourable geometries. To inject into the target orbit, an additional small manoeuvre may be needed. For NRHOs the required burn is typically in the order of a few meters per second.

Typical travel times for WSB transfers to NRHOs are between 90 and 160 days. Note that in practice, not a single WSB manoeuvre is planned. Instead, several deterministic burns and trajectory correction manoeuvres take place before and after apogee, to connect to the ideal trajectory towards the target orbit.

4.2 First guess generation

One of the initial scopes of the investigation was to reliably find preliminary WSB transfers, that can be used as initial guesses for successive optimisation and launch window definition. A suitable method for such purpose is the generation of natural transfers, i.e. without intermediate manoeuvres.

Starting from the target orbit, a small manoeuvre is added and the such-modified state is propagated backwards or forward in time. A reliable figure of merit to differentiate successful natural transfers is

the Earth proximity of the first perigee after WSB crossing. If the perigee radius is sufficiently low, the natural transfer is a suitable candidate to connect to an Earth parking orbit in subsequent steps. Example results of such a scan are shown in Figure 12.

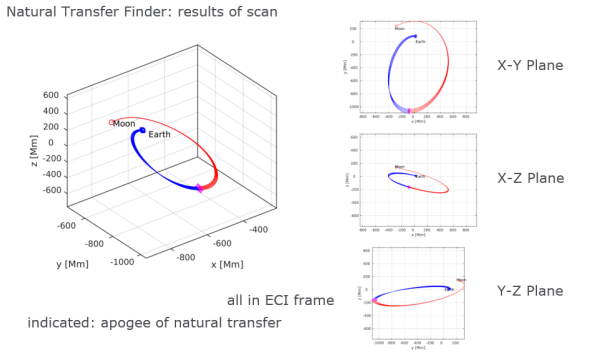

Figure 12: Natural transfers from Earth to NRHO, depicted in inertial frame in units of 1,000 km.

Experience shows that, in first approximation, perigees lower than 100,000 km provide acceptable results. Reducing this threshold generally improves the performance of the transfers but also risks discarding potentially suitable candidates. The mission designer may consider additional restrictions, such as a maximum allowable deviation of the perigee declination, or a variation of the natural transfer perigee epoch from the intended launch epoch. Finding reliable limit values for these parameters is a subject of ongoing investigations.

Figure 13 depicts the results of a numerical search for natural transfers as a function of manoeuvre direction in azimuth and elevation and using a fixed scan interval of manoeuvre magnitudes. As discussed above, the figure of merit to identify suitable manoeuvre directions is the number of natural transfers that reach Earth proximity.

Interestingly, the scan of the azimuth-elevation phase space presented the same circular patterns highlighted in the orbit strain analysis. In application, it was thus possible to restrict the search for WSB transfer with in-plane manoeuvres only. This resulted in numerical advantages for the local optimizer, reducing the number of variables and allowing a more efficient search, particularly for preliminary mission analysis phases where a large number of transfer options are to be investigated. Manoeuvre directions for which no or only a few natural transfers are identified can be readily discarded by a mission designer.

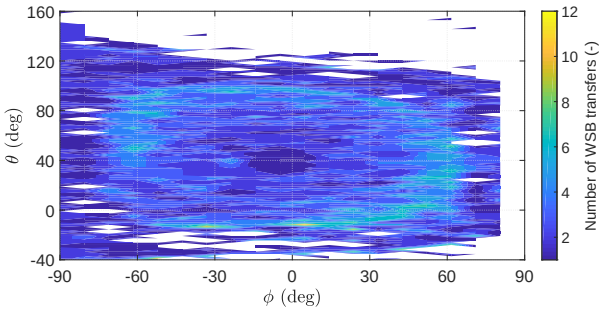

Figure 13: Search for natural transfers in azimuth-elevation space

4.3 Selection of launch windows

WSB transfers in general show a large variability and sensitivity to launch epoch and inclination. The exact transfer trajectory and its parameters depend on the geometry between Earth, Moon, and Sun. Naturally this restricts the launch window availability. In principle, WSB transfer opportunities repeat approximately every fourteen days. It is effectively always possible to find a WSB transfer within any fourteen-day period throughout the year. However, a transfer may be associated with a Δv cost exceeding the cost of a direct transfer. This nullifies the earlier-mentioned advantage of WSB transfers while retaining the generally disadvantageous long travel times. The largest share of a Δv increase lies in the WSB manoeuvre, as larger burns are required to match poor launch geometries.

In particular, for Earth orbits near the equator (i.e. with near-zero inclination), the available transfer windows for WSB transfers are limited to the equinoxes. Outside these favourable time windows, the departure orbit's apogee cannot easily match to a trajectory towards a lunar or libration point orbit.

Considering this, the results discussed above are not to be understood as a method to guarantee optimal transfers for any orbit geometry; the total Δv may be considerable if the Earth departure orbit connects poorly to the available natural transfers. However, restricting manoeuvre directions does offer an efficient way to generate first guess trajectories based on natural transfers.

5. Final remarks

The paper offered a preliminary analysis of escape dynamics in lunar non-Keplerian orbits, with specific application to NRHOs. The parameter space is investigated by applying a manoeuvre, using its magnitude

and direction as independent variables and creating visual maps, that help to define the solutions; a scalar metric is defined, borrowing the definition of strain from structural mechanics.

The analysis of the maps allows to identify regular and chaotic behaviours, the latter characterised by peaks and sudden variations in the parameter surface. The results strictly depend on integration time, although it is possible to make some long-term prediction after classifying the trajectories into families. The maps are meant as a preliminary tool, to generate initial guesses and identify transfer opportunities, prior to refining such solutions with local optimization.

A notable result is the existence of an optimal direction, in the Earth-Moon plane, for any kind of trajectory; i.e., given a desired type of transfer or escape, it is always possible to find a planar manoeuvre with minimum Δv that shows a strictly similar behaviour. Numerical evidence supports this statement, although a strict proof is not currently available; a preliminary hypothesis links such behaviour to the Earth-Moon-Sun geometry, at the manoeuvre epoch, and on the predominant role of the apparent Coriolis acceleration in non-Keplerian Earth-Moon orbits, leading to a lesser effect of the out-of-plane manoeuvre component.

Future studies will further investigate the trajectory sensitivity to manoeuvre direction, looking for a more solid proof of the numerical results, and attempt to provide a tool to predict long-term behaviours, while avoiding numerical propagation of the full trajectory.

Acknowledgements

The research was carried out at the European Space Operations Centre, under the Networking/Partnering Initiative (NPI) between Politecnico di Milano and ESA (author LB) and under the German Traineeship Program (GTP) between Deutsches Zentrums fr Luft- und Raumfahrt (DLR) and ESA (author AK).

References

[1] W. S. Koon, M. W. Lo, J. E. Marsden, and S. D. Ross, *Dynamical Systems, the Three-Body Problem and Space Mission Design*. Springer-Verlag, New York, 2007.

[2] E. Perozzi and S. Ferraz-Mello, *Space Manifold Dynamics*. Springer, 2010.

[3] C. R. Short, "Flow-informed strategies for trajectory design and analysis," Ph.D. Dissertation, Purdue University, 2016.

[4] N. Bosanac, *Leveraging natural dynamical structures to explore multi-body systems*. PhD Dissertation, 2016.

[5] C. R. Short and K. C. Howell, "Lagrangian coherent structures in various map representations for application to multi-body gravitational regimes," *Acta Astronautica*, Vol. 94, No. 2, 2014, pp. 592–607.

[6] V. Szebehely, *Theory of Orbits: The Restricted Problem of Three Bodies*. Academic Press, New York, 1967.

[7] V. Szebehely and G. Giacaglia, "On the elliptic restricted problem of three bodies," *The Astronomical Journal*, Vol. 69, 1964, p. 230.

[8] E. A. Belbruno, "Examples of the nonlinear dynamics of ballistic capture and escape in the Earth-Moon system," *Astrodynamics Conference*, 1990, p. 2896.

[9] E. A. Belbruno and J. K. Miller, "Sun-perturbed Earth-to-Moon transfers with ballistic capture," *Journal of Guidance, Control, and Dynamics*, Vol. 16, No. 4, 1993, pp. 770–775.

[10] D. A. Dei Tos and F. Topputo, "On the advantages of exploiting the hierarchical structure of astrodynamical models," *Acta Astronautica*, Vol. 136, 2017, pp. 236–247.

[11] D. Guzzetti, E. Zimovan, K. Howell, and D. Davis, "Stationkeeping Analysis for Spacecraft in Lunar Near Rectilinear Halo Orbits," *27th AAS/AIAA Space Flight Mechanics Meeting*, February 2017.

[12] K. Boudad, D. Davis, and K. Howell, "Disposal Trajectories from Near Rectilinear Halo Orbits," *AAS/AIAA Astrodynamics Specialist Conference*, February 2018.

[13] V. I. Oseledec, "A multiplicative ergodic theorem. Liapunov characteristic number for dynamical systems," *Trans. Moscow Math. Soc.*, Vol. 19, 1968, pp. 197–231.